# Two polaron flavors of the Bose-Einstein condensate impurity

A. A. Blinova,[1,2] M. G. Boshier,[1] and Eddy Timmermans[3]
[1] *P-21, Physics Division, Los Alamos National Laboratory, Los Alamos, New Mexico 87545, USA*
[2] *Department of Physics & Astronomy, Rice University, Houston, Texas 77251, USA*
[3] *T-4, Theory Division, Los Alamos National Laboratory, Los Alamos, New Mexico 87545, USA*
(Received 26 April 2013; published 8 November 2013)

We show that repulsive neutral-atom impurities in a dilute gas Bose-Einstein condensate (BEC) can self-localize in bubble polaron states formally analogous to electron bubbles in helium. The BEC is then the first impurity host medium known to exhibit both Landau-Pekar polaron states akin to that of self-localized electrons in a dielectric lattice and self-localized bubble polaron states. We find that the neutral BEC-impurity system is fully characterized by only two dimensionless coupling constants and that a single BEC impurity can be steered adiabatically from the Landau-Pekar to the bubble region. The adiabatic change is that of a crossover, not a transition.

DOI: 10.1103/PhysRevA.88.053610 PACS number(s): 67.85.Bc, 05.30.Jp, 03.75.Hh, 67.85.Hj

## I. INTRODUCTION

The polaron, a single distinguishable particle that interacts with the self-consistent deformation of the medium that contains it, is a paradigm of strong interaction physics in condensed matter [1,2], chemistry [3], and biophysics [4]. Polaron physics can now be studied in cold-atom systems [5]. Polarons self-localize when sufficiently cold and strongly coupled to the host medium. In nature, large [6] self-localized polarons appear in two flavors: particles that hardly deform the medium, such as electrons in dielectric lattices [7], and particles that greatly distort the medium, such as electron bubbles in condensed helium superfluids [8]. In the first class, the particle is accompanied by a cloud of small-amplitude collective excitations of the medium. We refer to this object [9,10] as a Landau-Pekar polaron. In the bubble systems, which occur in fluids and dense gases, the strongly repelling particle can be described as residing in a self-created cavity—the bubble—surrounded by fluid [11]. The effective mass and mobility of bubble and Landau-Pekar polarons exhibit quite different behaviors and so the two polaron flavors are customarily viewed as distinct. It is known that dilute gas Bose-Einstein condensates (BECs) [12,13] can localize impurities in Landau-Pekar polaron states [14,15]. We show below that impurities in a BEC can also form bubbles. This surprising discovery identifies a BEC as the first medium known to self-localize an impurity in both polaron flavors. Further, the system phase diagram presented here shows how the BEC-impurity polaron evolves continuously between the two regimes as the interaction strengths and BEC density are varied. The BEC-impurity system can then simulate large self-localized polarons in a boson environment [16]. In addition to direct BEC experiments, our bubble-crossover prediction can motivate a search for Landau-Pekar polarons in condensed fluids (the traditional hosts to bubbles) and may motivate a second look at fermion polarons. For example, can self-localized cold-atom fermion polarons [16] or self-localized protons in the dense neutron environment [17] of neutron star cores cross over to bubble states, thereby radically altering their properties?

## II. SYSTEM

We consider a neutral impurity atom of mass $m_I$ immersed in a homogeneous BEC of $N$ boson particles of mass $m_B$ contained in a macroscopic volume $\Omega$, giving an average density $\rho = N/\Omega$. Bosons at positions $\mathbf{r}$ and $\mathbf{r}'$ interact via a repulsive short-range interaction of scattering length $a_{BB}$, described by an effective potential $V_{BB}(\mathbf{r}-\mathbf{r}') = \lambda_{BB}\delta(\mathbf{r}-\mathbf{r}')$, where $\lambda_{BB} = (4\pi\hbar^2/m_B)a_{BB}$ and $a_{BB} > 0$. The boson chemical potential $\mu_B = \lambda_{BB}\rho$ sets the time scale $\hbar/\mu_B$ and the coherence length $\xi = 1/\sqrt{16\pi\rho a_{BB}}$ sets the length scale on which the BEC can respond to a perturbation. The perturbation here is provided by the impurity interacting with the bosons via $V_{IB}(\mathbf{r}-\mathbf{x}) = \lambda_{IB}\delta(\mathbf{r}-\mathbf{x})$, where $\mathbf{x}$ is the impurity position and the impurity-boson interaction strength $\lambda_{IB} = 2\pi\hbar^2(m_I^{-1}+m_B^{-1})a_{IB}$ is proportional to the impurity-boson scattering length $a_{IB}$, taken to be Feshbach tuned [18] to a large positive value [19]. We break the translational symmetry of the BEC-impurity system ground state by fixing the impurity center-of-mass position at $\mathbf{r}=0$ [20]. We write the BEC density in the presence of the impurity as $\rho_B(\mathbf{r}) = \rho + \delta\rho_B(\mathbf{r})$. Self-localization occurs when the effective potential $\lambda_{IB}\delta\rho_B(\mathbf{r})$ can trap the impurity.

## III. LANDAU-PEKAR POLARON

The impurity-boson repulsion can be simultaneously strong enough to self-trap the impurity and weak enough to hardly change the BEC density profile [Fig. 1(a)]. In this regime, the Bogoliubov expansion and transformation that describes the BEC fluctuations [21] can be carried out around the homogeneous BEC [22]. The interaction of the dilute BEC with an impurity of density $\rho_I(\mathbf{r}) = (2\pi)^{-3}\int d^3\mathbf{k}\, e^{i\mathbf{k}\cdot\mathbf{r}}\rho_{I,\mathbf{k}}$ then gives a Fröhlich Hamiltonian [23], familiar from electron-phonon interactions. Representing the quasiparticle annihilation and creation operators of momentum $\mathbf{k}$ and energy $\hbar\omega_k = \hbar k\sqrt{(1+\xi^2k^2)(\mu_B/m_B)}$ by $b_{\mathbf{k}}$ and $b_{\mathbf{k}}^\dagger$, respectively, the impurity-boson interaction is described by

$$H_{IB} = \frac{\lambda_{IB}}{\Omega}\sum_{\mathbf{k}}\rho_{I,-\mathbf{k}}\,\rho_{B,\mathbf{k}} \approx \lambda_{IB}\rho + \frac{M}{\sqrt{\Omega}}\sum_{\mathbf{k}}\nu_k\rho_{I,-\mathbf{k}}(b_{\mathbf{k}}^\dagger + b_{\mathbf{k}}), \qquad (1)$$

where $\rho_{B,\mathbf{k}}$ is the operator associated with the boson density. In Eq. (1), the impurity-phonon interaction matrix element

 

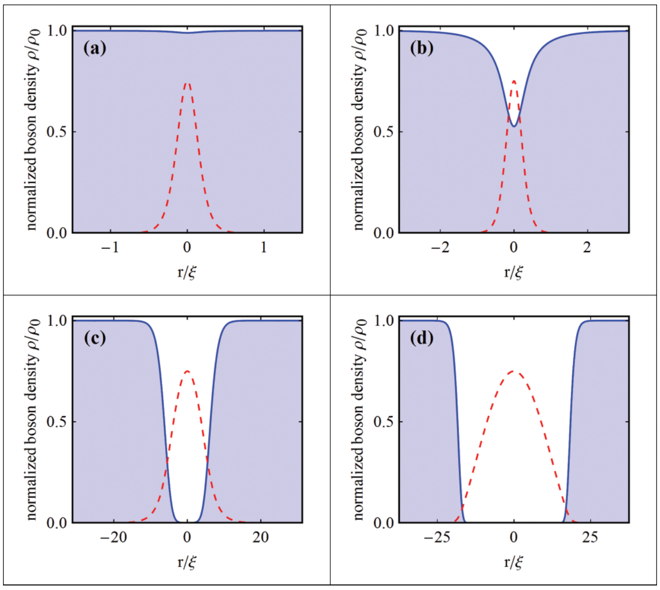


FIG. 1. (Color) Numerical results for the normalized boson density (blue shading) and un-normalized impurity wave function (red dashed line). The parameter values [see Eqs. (3) and (8)] are (a) $\beta = 25$ and $\alpha = 10^{-9}$, (b) $\beta = 25$ and $\alpha = 10^{-5}$, (c) $\beta = 25$ and $\alpha = 10^{1}$, and (d) $\beta = 5 \times 10^{4}$ and $\alpha = 10^{3}$.

$M = \lambda_{IB}\sqrt{\rho}$ and $\nu_k = (\xi^2 k^2/[1+\xi^2 k^2])^{1/4}$ is a structure factor arising from the Bogoliubov transformation. By showing that the Fröhlich coupling $H_{IB}$ amounts to a displacement of the **k**-mode oscillator coordinate $\phi_{\mathbf{k}} = (b^{\dagger}_{\mathbf{k}} + b_{-\mathbf{k}})/\sqrt{2}$, Landau and Pekar [10] integrated out the phonon modes. The resulting energy reduction takes the form of a self-interaction [22,24] $\Delta E = -M^2(2\pi)^{-3}\int d^3\mathbf{k}\, \rho_{I,-\mathbf{k}}\rho_{I,\mathbf{k}}(\nu_k^2/\hbar\omega_k)$, which in the strongly coupled regime overcomes the kinetic energy cost of localizing the impurity. Here the self-interaction potential is an attractive Yukawa potential of range $\xi$. It can cause self-localization when $\xi$ exceeds the impurity extent, which is comparable to [14]

$$R_o = \left[4\pi\rho a_{IB}^2(1+m_I/m_B)(1+m_B/m_I)\right]^{-1}. \qquad (2)$$

Specifically, when the ratio of the boson healing length $\xi$ to the self-localization length $R_o$

$$\beta = \frac{\xi}{R_o} = \sqrt{\pi\rho\frac{a_{IB}^4}{a_{BB}}}\left(1+\frac{m_I}{m_B}\right)\left(1+\frac{m_B}{m_I}\right) \geqslant 5, \qquad (3)$$

the above description predicts self-localization [14]. The binding energy, proportional to

$$E_o = \frac{\hbar^2}{2m_I R_o^2} = 2\left(\frac{m_B}{m_I}\right)\beta^2\mu_B, \qquad (4)$$

then significantly exceeds $\mu_B$. When scaled by $E_o$ and $R_o$, impurity observables in the Landau-Pekar regime depend only on the dimensionless coupling strength $\beta$ [14].

## IV. BUBBLE POLARON

When $a_{IB}$ grows sufficiently, numerical simulations discussed below show that the BEC is expelled from the impurity's vicinity [Figs. 1(c) and 1(d)]. We use Kuper's model of electron bubbles in helium [11] as the basis of a simple analytical treatment. The numerical results will show that this grossly simplified model works surprisingly well over a wide parameter range and also how it breaks down. With complete BEC and impurity separation [Fig. 1(d)] the impurity, trapped in a self-created spherical cavity of radius $R_c$ and volume $V_c$, has wave function $\chi(r) = (\sqrt{\pi R_c})^{-1}\sin(\pi r/R_c)/r$. Neglecting surface tension, the system energy difference $E_c$ with and without impurity is the impurity kinetic energy $\pi^2\hbar^2/2m_I R_c^2$ plus the energy cost of making the cavity $PV_c$, where $P = \lambda_{BB}\rho^2/2$ is the BEC pressure. Hence

$$E_c(R_c) = \frac{\pi^2\hbar^2}{2m_I R_c^2} + \frac{8\pi^2}{3}\frac{\hbar^2 a_{BB}}{m_B}\rho^2 R_c^3. \qquad (5)$$

The minimization $\partial E_c/\partial R_c = 0$ yields a stable bubble polaron state with cavity radius $R_c = [8(m_I/m_B)\rho^2 a_{BB}]^{-1/5}$ and impurity energy $E_c = (5/3)(\pi^2\hbar^2/2m_I R_c^2) = (5\pi/3)2^{-9/5}(m_B/m_I)^{3/5}\mu_B/(\sqrt{\rho a_{BB}^3})^{2/5}$.

## V. THE BEC PERMEABILITY

The qualitatively different BEC-impurity overlaps in Figs. 1(a) and 1(d) are caused by the difference in the relative importance of BEC "stiffness". In Fig. 1(a) the energy cost $E_x$ of removing $\Delta N = |\int d^3\mathbf{r}[\rho_B(\mathbf{r}) - \rho]|$ bosons from the impurity's vicinity exceeds the reduction in impurity-boson interaction energy, estimated as $E_o$ in the Landau-Pekar regime, whereas it is overwhelmed by $E_o$ in Fig. 1(d). Using $E_x = \Delta N\mu_B$ and estimating $\Delta N = |\lambda_{IB}/\lambda_{BB}|$ (see [25]) (valid in the Landau-Pekar and crossover regimes but not in the bubble regime), we introduce the ratio

$$\sigma = \frac{E_x}{E_o} = \left[4\pi\rho a_{IB}^3\left(1+\frac{m_I}{m_B}\right)^3\left(\frac{m_B}{m_I}\right)^2\right]^{-1} \qquad (6)$$

quantifying the relative importance of the displacement energy cost to the overlap energy gain of self-localization. We call this useful parameter the BEC-impurity permeability. In the Landau-Pekar regime, a direct analytical evaluation yields $|\delta\rho_B(\mathbf{r}=0)/\rho| = (4\sqrt{2}/3\sqrt{\pi})\sigma^{-1} = 1.064\sigma^{-1}$. Thus $\sigma \gg 1$ implies Landau-Pekar conditions where the repulsion is insufficient to overcome the BEC stiffness and displace the bosons noticeably [Fig. 1(a)]. A gradual increase in $a_{IB}$ then expels the bosons significantly when $\sigma \sim 1$ [Fig. 1(b)] and enters the large-depletion bubble limit [Figs. 1(c) and 1(d)] when $\sigma \ll 1$.

## VI. GENERAL CASE

A more general ground-state treatment, encompassing the Landau-Pekar and bubble regimes as limits, is based on the strong-coupling approximation of a many-body product state. Minimizing the energy while requiring the respective boson and impurity wave functions $\psi(\mathbf{r})$ and $\chi(\mathbf{r})$ to be normalized gives two coupled Gross-Pitaevskii equations

$$\begin{aligned}\mu_B\psi(\mathbf{r}) &= -\frac{\hbar^2\nabla^2}{2m_B}\psi(\mathbf{r}) + \lambda_{BB}|\psi(\mathbf{r})|^2\psi(\mathbf{r}) + \lambda_{IB}|\chi(\mathbf{r})|^2\psi(\mathbf{r}),\\ \epsilon_I\chi(\mathbf{r}) &= -\frac{\hbar^2\nabla^2}{2m_I}\chi(\mathbf{r}) + \lambda_{IB}|\psi(\mathbf{r})|^2\chi(\mathbf{r}),\end{aligned} \qquad (7)$$

where $\lim_{r\to\infty}\psi(r)=\sqrt{\rho}$ and $\mu_B$ and $\epsilon_I$ represent the Lagrange multipliers ensuring normalization $\int d^3\mathbf{r}|\psi(\mathbf{r})|^2 = N$ and $\int d^3\mathbf{r}|\chi(\mathbf{r})|^2 = 1$.

The BEC-impurity system has five physical parameters $m_B$, $m_I$, $\rho$, $a_{BB}$, and $a_{IB}$, but we find that the proper dimensional scaling of energies, density, and distances reveals a minimal dependence on just two coupling constants. The first is the length scale ratio $\beta = \xi/R_o$. The second is the mass-scaled boson gas parameter

$$\alpha = \left(\frac{m_B}{m_I}\right)\sqrt{\rho a_{BB}^3}. \tag{8}$$

All properly scaled observables can be cast in terms of $\alpha$ and $\beta$ [26]. For example, the permeability parameter $\sigma$ takes the form $\sigma(\alpha,\beta) = 1/4\pi^{1/4}\sqrt{\alpha\beta^3}$ and in the bubble limit the energy and cavity radius are given by $E_c = E_o(5\pi/24)\beta^2(4/\alpha)^{2/5}$ and $R_c = R_o 4\pi^{1/2}\beta\alpha^{1/5}$, respectively. To prove the minimal dependence, we substitute (real-valued) scaled dimensionless boson $p$ and impurity $g$ wave functions

$$\psi(\mathbf{r}) = \sqrt{\rho}\,p(\mathbf{x}=\mathbf{r}/\xi), \quad \chi(\mathbf{r}) = R_o^{-3/2} g(\mathbf{y}=\mathbf{r}/R_o) \tag{9}$$

into the coupled equations (7), scaling the energies and lengths to obtain the dimensionless form

$$\begin{aligned}\left(\nabla_x^2 + \frac{1-p^2(\mathbf{x})}{2}\right)p(\mathbf{x}) &= \frac{-4\pi\beta^2}{\sigma(\alpha,\beta)}g^2(\mathbf{y}=\mathbf{x}\beta)p(\mathbf{x}),\\ (\nabla_y^2 + e_I)g(\mathbf{y}) &= -\sigma(\alpha,\beta)p^2(\mathbf{x}=\mathbf{y}/\beta)g(\mathbf{y}),\end{aligned} \tag{10}$$

where $e_I = \epsilon_I/E_o$ and the $g$ and $p$ solutions have to satisfy the normalization $\int d^3\mathbf{y}\, g^2(\mathbf{y}) = 1$ and boundary condition $\lim_{x\to\infty} p(\mathbf{x}) = 1$.

To provide a rigorous test of the Landau-Pekar and bubble limiting behaviors and to study the intermediate regime for which there is no analytical treatment, we developed an algorithm to solve the coupled equations (7) numerically [27]. It yields the $\alpha$ and $\beta$ dependences of the relevant observables. For example, in Fig. 2 we plot the root-mean-square impurity extent $R_{\rm rms} = \sqrt{\int d^3\mathbf{r}\, r^2\rho_I(\mathbf{r})}$. On the left, the $\alpha$ independence of the Landau-Pekar impurity properties is confirmed by the zero slope of the curves, which also show the expected convergence to $R_{\rm rms} \approx 4.6R_0$ for $\beta \geqslant 20$ [14]. On the right, the straight lines of slope 1/5 confirm the expected bubble scaling $R_{\rm rms}/R_o \propto \beta\alpha^{1/5}$. The smooth change between these limits indicates a *crossover*, rather than a *transition*, between Landau-Pekar and bubble regimes.

Likewise, the relative BEC density change at the impurity position $|\delta\rho_B(\mathbf{r}=0)/\rho|$, plotted in Fig. 3, shows the $\sigma^{-1} \propto \alpha^{1/2}$ scaling of the Landau-Pekar polaron on the left side. Before crossing the line of unit relative density response, the curves level off and approach the bubble limit of maximal BEC depletion asymptotically. As in Fig. 2, the arrows on Fig. 3 illustrate that the crossovers occur near $\sigma = 1$. Figure 4 is the two-dimensional phase diagram for the system, produced by plotting $|\delta\rho_B(\mathbf{r}=0)/\rho|$ in the $(\alpha,\beta)$ plane, colored to show the polaron regimes and the region where the impurity-BEC

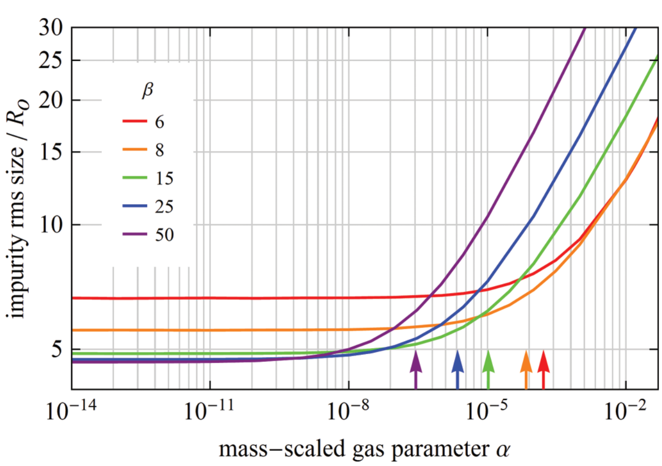


FIG. 2. (Color) Dependence on gas parameter $\alpha$ of the rms width of the impurity density (in units of scaled length $R_0$), for several values of the impurity-BEC interaction parameter $\beta$. For each $\beta$ arrows indicate the values of $\alpha$ for which permeability $\sigma = 1$.

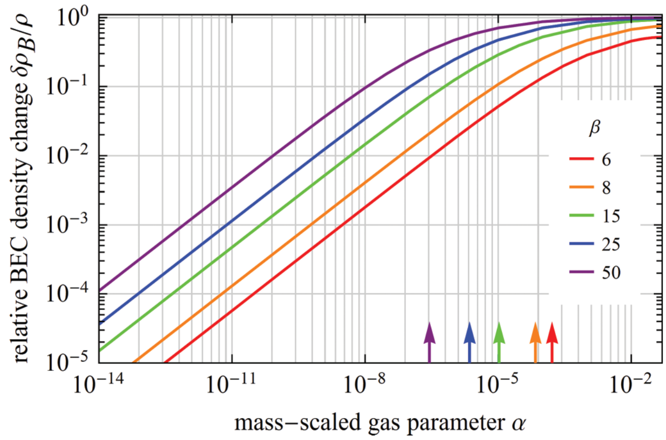


FIG. 3. (Color) Dependence on gas parameter $\alpha$ of the relative decrease in BEC density at the impurity location, for several values of the impurity-BEC interaction parameter $\beta$. For each $\beta$ arrows indicate the values of $\alpha$ for which permeability $\sigma = 1$.

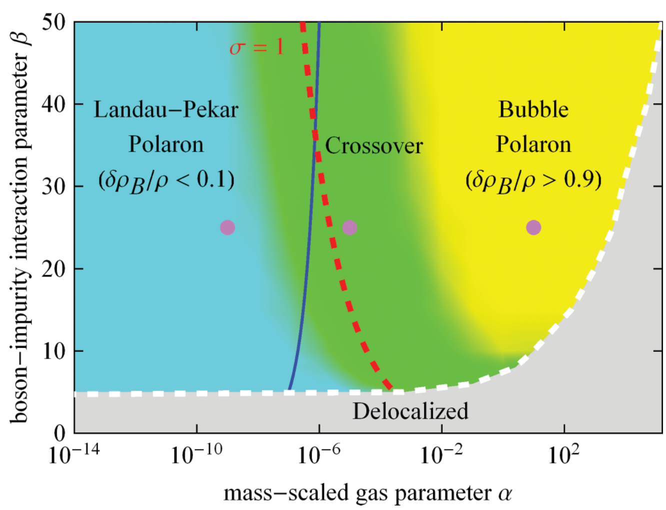


FIG. 4. (Color) Phase diagram of the BEC-impurity system obtained as a plot of $|\delta\rho_B(\mathbf{r}=0)/\rho|$. The dots in the Landau-Pekar, crossover, and bubble regions correspond to the BEC density profiles in Figs. 1(a), 1(b), and 1(c), respectively. The blue line is a trajectory that tunes the system continuously from the Landau-Pekar limit to the bubble limit (off the top of the plot).

interaction is not strong enough to cause self-localization. The red $\sigma = 1$ line lies, as expected, on top of the crossover region.

## VII. EXPERIMENTAL REALIZATION

The remarkable ability of a BEC to self-localize impurities both in Landau-Pekar and in bubble states could be strikingly illustrated by an experiment that adiabatically Feshbach-tunes the same BEC-impurity system from one limit to the other. For typical densities ($10^{11}$ cm$^{-3} < \rho < 10^{14}$ cm$^{-3}$) and realistic ranges for $a_{BB}$ and $m_B/m_I$, we find that cold-atom $\alpha$ values may range from $10^{-7}$ to $10^{-1}$. Increasing $a_{IB}$ by Feshbach tuning could achieve self-localization at $\beta \sim 5$ (see Fig. 4). Using Eq. (3) and scaling scattering lengths and densities by the typical values of 1 nm and $\overline{\rho} = 10^{13}$ cm$^{-3}$, this corresponds to $a_{IB} = a_{IB}^{\mathrm{SL}}$, where

$$a_{IB}^{\mathrm{SL}} = \frac{168\ \mathrm{nm}}{\sqrt{\left(1+\frac{m_B}{m_I}\right)\left(1+\frac{m_I}{m_B}\right)}}\left(\frac{a_{BB}/\mathrm{nm}}{\rho/\overline{\rho}}\right)^{1/4}. \tag{11}$$

This self-localization near $\beta \sim 5$ results in a Landau-Pekar polaron if $\sigma = (4\pi^{1/4}\sqrt{125\alpha})^{-1} \gg 1$, requiring

$$a_{BB} \ll 2.00\ \mathrm{nm}\,(\rho/\overline{\rho})^{-1/3}(m_B/m_I)^{-2/3}\,. \tag{12}$$

A further increase in $a_{IB}$ and/or $\rho$ can lower the permeability and effect a cross over to the bubble regime when $a_{IB} \sim a_{IB}^{\mathrm{cross}}$, where from Eq. (6)

$$a_{IB}^{\mathrm{cross}} = 200\ \mathrm{nm}\frac{(\rho/\overline{\rho})^{-1/3}(m_B/m_I)^{-2/3}}{(1+m_I/m_B)}. \tag{13}$$

Throughout, the permeability parameter varies as

$$\sigma = \frac{1.68}{\left(a_{IB}/\overline{a}_{IB}^{\mathrm{SL}}\right)^3}\frac{1}{(\rho/\overline{\rho})^{1/4}}\frac{1}{(a_{BB}/1\ \mathrm{nm})^{3/4}}\left(\frac{m_B}{m_I}\right)^{-1/2}, \tag{14}$$

where $\overline{a}_{IB}^{\mathrm{SL}}$ denotes the scattering length of Eq. (11) at standard density $\rho = \overline{\rho}$. The adiabatic ($a_{IB}$,$\rho$) variation traces out a trajectory on the phase diagram (e.g., blue line on Fig. 4) that starts in the low-$\alpha$, cyan-colored, Landau-Pekar region. An increase in BEC density and a Feshbach increase in $a_{IB}$ can then, eventually, steer the BEC-impurity across the crossover regime into the yellow-colored bubble region.

We now consider two potential issues facing such an experiment. The first is the lifetime of the impurity against three-body recombination. An increase in $a_{IB}$ is generally [but not always (see below)] accompanied by a decrease in lifetime [28]. Estimating the three-body limited impurity lifetime $\tau_I$ as in [29], we expect $\tau_I^{\mathrm{est}} \sim (\sqrt{3}/3.9)[\sqrt{1+2(m_B/m_I)}(\hbar/m_B)a_{IB}^4\rho^2]^{-1}$. As the time scale of the BEC response (and the slowest time scale in the system), we expect $\tau_B = \hbar/\mu_B$ to set the scale of the self-localization dynamics. The estimated impurity lifetime with full overlap can then significantly exceed $\tau_B$ as long as $\beta$ is not too large,

$$\tau_I^{\mathrm{est}} = \tau_B\frac{4\pi^2}{\beta^2}\frac{\sqrt{3}}{3.9}\frac{(1+m_I/m_B)^2(1+m_B/m_I)^2}{\sqrt{1+2m_B/m_I}}. \tag{15}$$

A more careful study of the three-body loss [30] found that $\tau_I^{\mathrm{est}}$ should be divided by an oscillating Stuckelberg factor related to three-body Efimov physics [31]. Near the nodes of the Stuckelberg factor the lifetime greatly increases. Further, the nearly complete separation of the impurity and the BEC in the bubble limit implies a significant increase in impurity lifetime for sufficiently large $a_{IB}$ because the three-body recombination loss rate is proportional to the overlap $\int d^3\mathbf{r}\,\rho_B^2(\mathbf{r})\rho_I(\mathbf{r})$. We note that in condensed helium, the increased lifetime of positronium [32,33] has been used as a signal of self-localization [34].

The second challenge faced by a bubble polaron experiment may be the buoyancy force $\mathbf{F} = -\nabla E_c(\rho) = -(4/5)E_c(\nabla\rho)/\rho$ attempting to expel the impurity from the high-density region in an inhomogeneous BEC. A two-color trap or a species specific potential [35,36] may be necessary to keep the impurity bubble in place. We note that while the bubble polaron always seeks low BEC density, the Landau-Pekar polaron can be high-density seeking.

## VIII. CONCLUSION

We have shown that a distinguishable neutral atom embedded in a dilute BEC can, if the BEC-impurity repulsion is strong enough, self-localize in a bubble polaron state in which the impurity is impermeable to the condensate. The BEC is therefore the first host medium known that can localize impurities as both Landau-Pekar and bubble polarons. We introduced a single parameter $\sigma$, called the permeability, that characterizes the overlap of the self-localized impurity with the host fluid: Its value ranges from $\sigma \gg 1$ in the Landau-Pekar limit to $\sigma \ll 1$ in the bubble limit. We have shown that the BEC-impurity system is fully characterized by just two dimensionless coupling constants. In the corresponding phase diagram, the bubble and Landau-Pekar states correspond to broad regions that are separated by a smooth crossover region near $\sigma \sim 1$. Finally, we pointed out that a single impurity-BEC system can be experimentally steered from one regime to the other.


## ACKNOWLEDGMENTS

E.T. would like to thank the Aspen Center for Physics for a visit, during which part of this work was conceived. This work was partially funded by the Los Alamos National Laboratory LDRD Program.



[1] *Polarons in Ionic Crystals and Polar Semiconductors*, edited by J. T. Devreese (North-Holland, Amsterdam, 1972).

[2] N. N. Bogolubov and N. N. Bogolubov, Jr., *Polaron Theory: Model Problems* (Gordon and Breach, Amsterdam, 2000).

[3] J. L. Bredas and G. B. Street, Acc. Chem. Res. **18**, 309 (1985).

[4] E. M. Conwell, Proc. Natl. Acad. Sci. USA **102**, 8795 (2005).

[5] We believe that the first mention of polaron physics in a cold-atom context was in L. Mathey, D. W. Wang, W. Hofstetter, M. D. Lukin, and E. Demler, Phys. Rev. Lett. **93**, 120404 (2004).

[6] Large polarons have a size that significantly exceeds the lattice constant when the medium is a lattice, in contrast to the lattice polarons discussed in M. Bruderer, A. Klein, S. R. Clark, and D. Jaksch, Phys. Rev. A **76**, 011605 (2007); V. M. Stojanović, T. Shi, C. Bruder, and J. I. Cirac, Phys. Rev. Lett. **109**, 250501 (2012); A. Mezzacapo, J. Casanova, L. Lamata, and E. Solano, *ibid*. **109**, 200501 (2012).
[7] J. T. Devreese, in *Encyclopedia of Applied Physics*, edited by G. L. Trigg (VCH, Weinheim, 1996), Vol. 14, p. 383.
[8] J. P. Hernandez, Rev. Mod. Phys. **63**, 675 (1991).
[9] L. D. Landau, Phys. Z. Sowjetunion **3**, 644 (1933).
[10] L. D. Landau and S. I. Pekar, Zh. Eksp. Teor. Fiz. **18**, 419 (1948).
[11] C. G. Kuper, Phys. Rev. **122**, 1007 (1961).
[12] M. H. Anderson, J. R. Ensher, M. R. Matthews, C. E. Wieman, and E. A. Cornell, Science **269**, 198 (1995).
[13] K. B. Davis, M. O. Mewes, M. R. Andrews, N. J. van Druten, D. S. Durfee, D. M. Kurn, and W. Ketterle, Phys. Rev. Lett. **75**, 3969 (1995).
[14] F. M. Cucchietti and E. Timmermans, Phys. Rev. Lett. **96**, 210401 (2006).
[15] R. M. Kalas and D. Blume, Phys. Rev. A **73**, 043608 (2006).
[16] Recently, cold-atom experiments have realized polarons in a fermion environment; see A. Schirotzek, C.-H. Wu, A. Sommer, and M. W. Zwierlein, Phys. Rev. Lett. **102**, 230402 (2009); C. Kohstall, M. Zaccanti, M. Jag, A. Trenkwalder, P. Massignan, G. M. Bruun, F. Schreck, and R. Grimm, Nature (London) **485**, 615 (2012).
[17] M. Kutschera and W. Wójcik, Phys. Rev. C **47**, 1077 (1993).
[18] C. Chin, R. Grimm, P. Julienne, and E. Tiesinga, Rev. Mod. Phys. **82**, 1225 (2010).
[19] Feshbach tuning to $a_{IB} \ll 0$ gives metastable polaron states; see M. Bruderer, W. Bao, and D. Jaksch, Europhys. Lett. **82**, 30004 (2008).
[20] The true ground state preserves the translational symmetry, but the symmetry-breaking energy cost is negligible in the strong-coupling limit.
[21] N. Bogoliubov, J. Phys. U.S.S.R. **11**, 23 (1947).
[22] D. H. Santamore and E. Timmermans, New J. Phys. **13**, 103029 (2011).
[23] H. Fröhlich, Adv. Phys. **3**, 325 (1954).
[24] W. Casteels, T. Cauteren, J. Tempere, and J. T. Devreese, Laser Phys. **21**, 1480 (2011).
[25] P. Massignan, C. J. Pethick, and H. Smith, Phys. Rev. A **71**, 023606 (2005).
[26] $\beta$ and $\sigma$ can also be used as coupling parameters, but we prefer to use $\alpha$ because tuning $a_{IB}$ leaves $\alpha$ unchanged.
[27] A. A. Blinova, E. Timmermans, and M. G. Boshier (unpublished).
[28] S. Inouye, M. R. Andrews, J. Stenger, H. J. Miesner, D. M. Stamper-Kurn, and W. Ketterle, Nature (London) **392**, 151 (1998).
[29] P. O. Fedichev, M. W. Reynolds, and G. V. Shlyapnikov, Phys. Rev. Lett. **77**, 2921 (1996).
[30] B. D. Esry, C. H. Greene, and J. P. Burke, Phys. Rev. Lett. **83**, 1751 (1999).
[31] J. Wang, J. P. D'Incao, B. D. Esry, and C. H. Greene, Phys. Rev. Lett. **108**, 263001 (2012).
[32] D. A. L. Paul and R. L. Graham, Phys. Rev. **106**, 16 (1957).
[33] J. Wackerle and R. Stump, Phys. Rev. **106**, 18 (1957).
[34] R. A. Ferrell, Phys. Rev. **108**, 167 (1957).
[35] J. Catani, G. Barontini, G. Lamporesi, F. Rabatti, G. Thalhammer, F. Minardi, S. Stringari, and M. Inguscio, Phys. Rev. Lett. **103**, 140401 (2009).
[36] G. Lamporesi, J. Catani, G. Barontini, Y. Nishida, M. Inguscio, and F. Minardi, Phys. Rev. Lett. **104**, 153202 (2010).